



## Unaccounted variability in NH<sub>3</sub> agricultural sources detected by IASI contributing to European spring haze episode

Audrey Fortems-Cheiney, Gaëlle Dufour, Lynda Hamaoui-Laguel, Gilles Foret, Guillaume Siour, M. van Damme, Frédérik Meleux, Pierre-François Coheur, Cathy Clerboux, Lieven Clarisse, et al.

### ► To cite this version:

Audrey Fortems-Cheiney, Gaëlle Dufour, Lynda Hamaoui-Laguel, Gilles Foret, Guillaume Siour, et al.. Unaccounted variability in NH<sub>3</sub> agricultural sources detected by IASI contributing to European spring haze episode. *Geophysical Research Letters*, 2016, 43 (10), pp.5475-5482. 10.1002/2016GL069361 . insu-01322800

**HAL Id: insu-01322800**

**<https://insu.hal.science/insu-01322800>**

Submitted on 19 Jul 2020

**HAL** is a multi-disciplinary open access archive for the deposit and dissemination of scientific research documents, whether they are published or not. The documents may come from teaching and research institutions in France or abroad, or from public or private research centers.

L'archive ouverte pluridisciplinaire **HAL**, est destinée au dépôt et à la diffusion de documents scientifiques de niveau recherche, publiés ou non, émanant des établissements d'enseignement et de recherche français ou étrangers, des laboratoires publics ou privés.



## RESEARCH LETTER

10.1002/2016GL069361

## Key Points:

- Strong potential of IASI for deducing NH<sub>3</sub> daily emissions
- High NH<sub>3</sub> emissions revealed over central Europe
- Strong impact of NH<sub>3</sub> emissions on pollution particle formation

## Supporting Information:

- Supporting Information S1

## Correspondence to:

A. Fortems-Cheiney,  
audrey.fortems@lscce.ipsl.fr

## Citation:

Fortems-Cheiney, A., et al. (2016), Unaccounted variability in NH<sub>3</sub> agricultural sources detected by IASI contributing to European spring haze episode, *Geophys. Res. Lett.*, 43, 5475–5482, doi:10.1002/2016GL069361.

Received 28 APR 2016

Accepted 7 MAY 2016

Accepted article online 11 MAY 2016

Published online 23 MAY 2016

Unaccounted variability in NH<sub>3</sub> agricultural sources detected by IASI contributing to European spring haze episode

A. Fortems-Cheiney<sup>1,2</sup>, G. Dufour<sup>1</sup>, L. Hamaoui-Laguel<sup>2</sup>, G. Foret<sup>1</sup>, G. Siour<sup>1</sup>, M. Van Damme<sup>3</sup>, F. Meleux<sup>2</sup>, P.-F. Coheur<sup>3</sup>, C. Clerbaux<sup>3,4</sup>, L. Clarisse<sup>3</sup>, O. Favez<sup>2</sup>, M. Wallasch<sup>5</sup>, and M. Beekmann<sup>1</sup>
<sup>1</sup>Laboratoire Interuniversitaire des Systèmes Atmosphériques, CNRS/INSU, UMR 7583, Université Paris-Est Créteil et Université Paris Diderot, Institut Pierre Simon Laplace, Créteil, France, <sup>2</sup>Institut National de l'Environnement et des Risques Industriels (INERIS), Verneuil-en-Halatte, France, <sup>3</sup>Spectroscopie de l'atmosphère, Chimie Quantique et Photophysique, Université Libre de Bruxelles, Brussels, Belgium, <sup>4</sup>LATMOS/IPSL, UPMC Université Paris 06, Sorbonne Universités, UVSQ, CNRS, Paris, France, <sup>5</sup>Umweltbundesamt, Langen, Germany

**Abstract** Ammonia (NH<sub>3</sub>), whose main source in the troposphere is agriculture, is an important gaseous precursor of atmospheric particulate matter (PM). We derived daily ammonia emissions using NH<sub>3</sub> total columns measured from the Infrared Atmospheric Sounding Interferometer (IASI) on board Metop-A, at a relatively high spatial resolution (grid cell of 0.5° × 0.5°). During the European spring haze episodes of 24–31 March 2012 and 8–15 March 2014, IASI reveals NH<sub>3</sub> total column magnitudes highlighting higher NH<sub>3</sub> emissions over central Europe (especially over Germany, Czech Republic, and eastern France) from the ones provided by the European reference European Monitoring and Evaluation Programme inventory. These ammonia emissions exhibit in addition a large day-to-day variability, certainly due to spreading practices. The increase of NH<sub>3</sub> emissions in the model, that reaches +300% locally, leads to an increase of both NH<sub>3</sub> and PM<sub>2.5</sub> surface concentrations and allows for a better comparison with independent measurements (in terms of bias, root-mean-square error, and correlation). This study suggests that there are good prospects for better quantifying NH<sub>3</sub> emissions by atmospheric inversions.

## 1. Introduction

Since several years, particulate matter pollution events occur in late winter or early spring with PM<sub>10</sub> (particulate matter with an aerodynamic diameter less than 10 μm) daily mean concentrations exceeding the alert threshold of 80 μg m<sup>-3</sup> over large parts of Europe (i.e., in March 2012, April 2013, March 2014, and March 2015). These specific spring events are often linked with favorable anticyclonic conditions and high ammonium nitrate (NH<sub>4</sub>NO<sub>3</sub>) surface concentrations, suggesting the importance of gaseous precursor emissions and in particular those of ammonia NH<sub>3</sub> [Erisman et al., 2008], whose main atmospheric source is agriculture. The sensitivity of NH<sub>4</sub>NO<sub>3</sub> formation with respect to precursor gases in air quality models crucially depends on the correct simulation of precisely the precursor gases [Bessagnet et al., 2014; Petetin et al., 2015]. Despite this, ammonia is the most poorly monitored pollutant regulated by European directives for air quality (e.g., no monitoring of NH<sub>3</sub> in Air Quality Directive 2008/50/EC), for several reasons.

First, the measurement of this compound at the surface is challenging at relevant mixing ratios (<10 ppbv) [von Bobutski et al., 2010; Hertel et al., 2012], and only few countries maintain an operational network (i.e., National Air Quality Monitoring Network (LML in Dutch) and the Measuring Ammonia in Nature MAN in the Netherlands, National Ammonia Monitoring Network NAMN in UK). As a result, there is no extended and operational measurement network for NH<sub>3</sub> at the European scale as for other air pollutants (such as ozone, PM<sub>10</sub>, and PM<sub>2.5</sub>) and international monitoring strategies are restricted to a few campaigns [e.g., Flechard et al., 2011].

Second, quantification of NH<sub>3</sub> emission fluxes with an inventory-based approach is subject to high uncertainty. At the European scale, reference NH<sub>3</sub> emissions are provided in the European Monitoring and Evaluation Programme (EMEP) inventory [Vestreng, 2003], using national annual declarations and applying emission factors, the uncertainty of the latter being usually estimated between 100 and 300% [European Monitoring and Evaluation Programme/European Environment Agency, 2009]. In addition, preprocessing of EMEP anthropogenic emissions includes spatial regridding and temporal disaggregation [Menut et al., 2012]: smooth seasonal, weekly,

and hourly profiles are used to get hourly emissions from annual totals, but these time profiles are not adapted to ammonia [Menut *et al.*, 2012], for which a dynamical approach is required. Indeed, ammonia emissions depend on a variety of physicochemical processes in the soil and the interface to the atmosphere (leaching of fertilizer into the soil by rain, solubility as a function of pH, volatilization as a function of temperature, and wind), which in turn depend on meteorological conditions and soil properties as well as on agricultural practices [Skjøth *et al.*, 2011; Hamaoui-Laguel *et al.*, 2014]. These ammonia agricultural sources fall into two main categories: animal husbandry and manure/fertilizer spreading, the first one accounting for more than 80% of European  $\text{NH}_3$  emissions [Hutchings *et al.*, 2009]. Even with a lower contribution to the annual total of European  $\text{NH}_3$  emissions, spreading emissions are still critical and are of particular interest, as they are enhanced over small time periods, especially during a few weeks at the end of winter or in early spring. For example, 90% of the mineral fertilizer is applied over Danish winter wheat in spring, when growth starts [Skjøth *et al.*, 2004]. However, the exact timing of fertilizer spreading is difficult to predict, as it also depends on agricultural practices and meteorological conditions, and is therefore not taken into account in the temporal disaggregation of the existing emission inventories.

Several studies aimed at improving these ammonia inventories, by developing more detailed emission models taking into account among others exact location of farm houses, number of livestock, fertilization rates, and dates of spreading (e.g., for Denmark [Skjøth *et al.*, 2004], for UK [Hellsten *et al.*, 2008], and for France [Hamaoui-Laguel *et al.*, 2014]). Remaining limitations come from the fact that detailed agricultural data (i) are not publicly available due to confidentiality, (ii) are not available in most of the European countries, and (iii) do not exist for all years (e.g., French data are only available every 6 years [AGRESTE, Service Central d'Enquêtes et d'Études Statistiques, 2006]).

In this context, and as an alternative to direct emission modeling, attempts have been made to develop complementary inverse approaches, in order to deduce  $\text{NH}_3$  emissions from satellite observations. Zhu *et al.* [2013] have first considered the potential of the Tropospheric Emission Spectrometer (TES) instrument to constrain monthly ammonia emissions for the U.S. Here we take advantage of the high spatial and temporal coverage of  $\text{NH}_3$  distributions offered by the Infrared Atmospheric Sounding Interferometer (IASI) instrument [Clarisse *et al.*, 2009] to derive European  $\text{NH}_3$  emissions with a better resolution (grid cell of  $0.5^\circ \times 0.5^\circ$ , at a daily scale). One of the objectives is the quantification of  $\text{NH}_3$  emissions due to spreading practices at the European scale. To evaluate the impact of agricultural  $\text{NH}_3$  emissions on particulate matter, we have focused our efforts on two representative spring particle pollution events: 24–31 March 2012 and 8–15 March 2014. For example, station JonvilleenWoevre located over agricultural region in East of France showed peak  $\text{PM}_{2.5}$  values in the range of  $40\text{--}60 \mu\text{g m}^{-3}$  each March over 2011–2015 ([www.prevair.org](http://www.prevair.org); [www.air-lorraine.org](http://www.air-lorraine.org)), which is comparable to the two examples shown here.

## 2. Data Set/Tools

### 2.1. Chemistry Transport Model CHIMERE for Air Quality Assessment

The chemistry transport model (CTM) used in this study to simulate hourly concentrations for a large set of pollutants is the regional model CHIMERE version 2013a [Menut *et al.*, 2013]. This model is driven by the European Centre for Medium-Range Weather Forecasts global meteorological fields. The horizontal resolution is given as follows:  $0.5^\circ \times 0.5^\circ$  over  $14^\circ\text{W}/25.5^\circ\text{E}$ – $35^\circ\text{N}/58^\circ\text{N}$ . The vertical grid contains 17 layers from surface to 200 hPa. Given a set of  $\text{NH}_3$ ,  $\text{NO}_x$ ,  $\text{SO}_x$ , volatile organic compounds, and CO emissions, CHIMERE calculates the concentrations of 28 gas phase and 16 aerosol species [Menut *et al.*, 2013], including  $\text{NH}_3$ . For inorganic species, aerosol thermodynamic equilibrium is achieved using the ISORROPIA model [Nenes *et al.*, 1999]. Two sets of simulations have been performed with CHIMERE: one with  $\text{NH}_3$ -EMEP reference emissions (as seen in Figure 1a) and the second with  $\text{NH}_3$ -SAT emissions deduced from IASI observations. In order to have a sufficient spin-up for  $\text{PM}_{2.5}$  concentrations to build-up and to allow meaningful evaluation of  $\text{NH}_3$  concentrations against weekly German sites (in March 2014), as described in the following, runs were performed from 18 to 31 March 2012 and from 1 to 19 March 2014.

### 2.2. IASI $\text{NH}_3$ Total Columns

As part of Metop-A, the IASI instrument has been flying on a low Sun-synchronous polar orbit since October 2006, with equator crossing times of 09:30 and 21:30 LST [Clerbaux *et al.*, 2009]. The algorithm used to retrieve

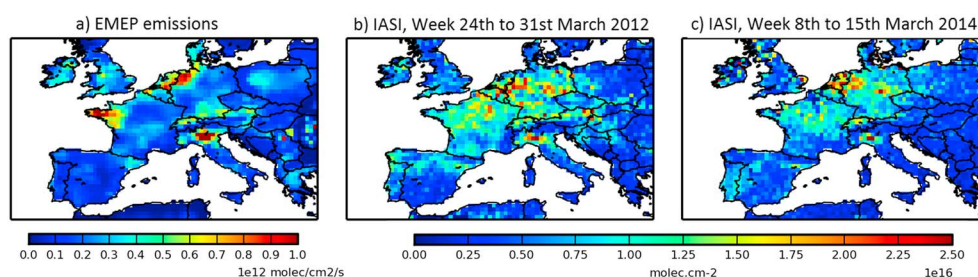


**Figure 1.** (a) Mean weekly EMEP  $\text{NH}_3$  reference emissions at 10:00 LST from 24 to 31 March 2012 and from 8 to 15 March 2014, in  $10^{12}$  molecules  $\text{cm}^{-2} \text{s}^{-1}$ . IASI  $\text{NH}_3$  weekly mean (in  $10^{16}$  molecules  $\text{cm}^{-2}$ ) (b) from 24 to 31 March 2012 and (c) from 8 to 15 March 2014. IASI land pixels are averaged into super-observations at the  $0.5^\circ \times 0.5^\circ$  spatial resolution.

$\text{NH}_3$  columns from the radiance spectra is described in Van Damme *et al.* [2014a]. In this study, we only consider land measurements from the morning overpass, which were recently evaluated against surface measurements and aircraft campaigns [Van Damme *et al.*, 2015a] and which are generally more sensitive to  $\text{NH}_3$  because of higher thermal contrast [Van Damme *et al.*, 2014a]. The potential of IASI to provide information at high temporal resolution, up to daily scale, is sometimes hampered by (i) the cloud coverage as only observations with a cloud coverage lower than 25% are processed and (ii) large retrieval errors, which are driven by low thermal contrast and/or low amounts of  $\text{NH}_3$  [Van Damme *et al.*, 2014a]. Here IASI total columns are averaged into “super-observations” (average of all IASI data within the  $0.5^\circ \times 0.5^\circ$  resolution of CHIMERE). It is important to note that we applied a sharp selection to the IASI super-observations: to assure the robustness of the IASI signal, we only selected IASI pixels for which the retrieval error does not exceed 50%. The numbers of selected IASI super-observations is presented in Table S1 in the supporting information.

### 3. Case Study of the March 2012 and of March 2014 Pollution Episodes

From 24 to 31 March 2012 and from 8 to 15 March 2014, widespread particulate matter pollution episodes affected Northwestern Europe. During both periods, extreme  $\text{PM}_{2.5}$  concentrations were observed in Belgium and in eastern France where several measurements from the air quality database system of the European Environmental Agency AirBase exceeded  $100 \mu\text{g m}^{-3}$ . These pollution events were associated with (i) no precipitation over almost all of Europe leading to an absence of wet deposition, (ii) cold nights conducive to thermal inversions that hampered pollution dispersion, and (iii) highly stable and low northeasterly winds (wind speed of 15 km/h at maximum over land, all over Europe). During these weeks and thanks to favorable meteorological conditions, IASI offers reliable daily measurements. These show strong day-to-day variability, highly correlated to daily  $\text{PM}_{2.5}$  surface observations (mean spatiotemporal correlation  $r=0.75$  over Belgium;  $r=0.79$  over the French region Champagne-Ardenne from 8 to 15 March 2014, not shown).

The highest EMEP emissions are located over four regions (the Netherlands, the Po and the Ebro Valleys, and the French region Brittany, see Figure 1a), known as major European animal husbandry sources [Van Damme *et al.*, 2014b]. In contrast and as seen in Figures 1b and 1c, IASI land super-observations for the two concerned episodes reveal high  $\text{NH}_3$  levels over central Europe (particularly over Germany and east of France and also over Poland, Czech Republic, etc.). Such a specific spatial distribution over agricultural regions combined with a high day-to-day variability suggests  $\text{NH}_3$  due to punctual spreading practices that are not represented in the EMEP inventory. We then used a typical method to relate IASI  $\text{NH}_3$  total columns to  $\text{NH}_3$  surface emissions, assuming that transport to neighboring cells is negligible. A sensitivity test, showing that  $\text{NH}_3$  columns are by far largest in the grid box corresponding to emissions (70% of  $\text{NH}_3$  columns, at least, are from the grid box corresponding to the emissions), and strong correlations between total columns and emissions (often higher than 0.6, as seen in Tables S2 and S3 and in Figure S3), confirm the robustness of our method during the studied periods. The detailed description and evaluation of such method can be found in the supporting information. The resulting emissions are referred to  $\text{NH}_3$ -SAT emissions in the following.

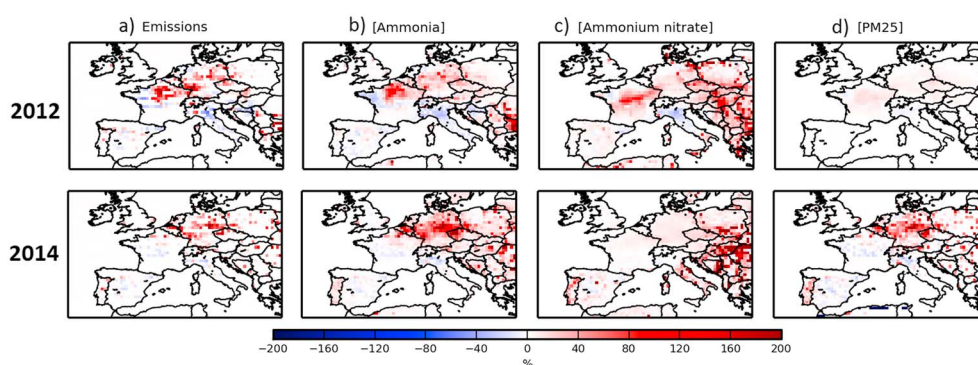


**Figure 2.** Mean weekly relative differences of (a)  $\text{NH}_3$ -SAT emissions compared to EMEP, (b) ammonia concentrations simulated using  $\text{NH}_3$ -SAT against EMEP emissions, (c) ammonium nitrate concentrations simulated using  $\text{NH}_3$ -SAT against EMEP emissions, and (d)  $\text{PM}_{2.5}$  concentrations simulated using  $\text{NH}_3$ -SAT against EMEP emissions. (top) From 24 to 31 March 2012 and (bottom) from 8 to 15 March 2014. Units in percent.

## 4. Results

### 4.1. Redistribution of European $\text{NH}_3$ Emissions

Figure 2a displays the relative difference of  $\text{NH}_3$ -SAT emissions deduced from IASI from 18 to 31 March 2012 and from 8 to 15 March 2014 compared to EMEP. The emissions constrained with IASI reveal additional emissions over central Europe, especially over Germany and east of France, and to a lesser extent over eastern Europe, especially over Poland and Czech Republic. As an example, high  $\text{NH}_3$ -SAT emissions, increased by 300% compared to EMEP at the grid cell scale, are deduced from IASI in the Magdeburg area in Germany (see Figure S4, on 24, 26, and 28 March 2012 and on 8, 11, 13, and 14 March 2014), known for its high level production of beet sugar and wheat. Over Czech Republic, large increases of emissions are seen for 25 and 26 March 2012 and for 8 and 14 March 2014. Over eastern France, the increase of emissions is particularly seen for 25, 27, and 28 March 2012 and for 12 March 2014 (see Figure S4).

This new  $\text{NH}_3$  spatial distribution of emissions is in qualitative agreement with recently published studies. The high values over east of France are consistent with the model study of Hamaoui-Laguel *et al.* [2014] and their improved representation of  $\text{NH}_3$  emissions due to mineral fertilizer spreading for France, which are particularly due to wheat, barley, sugar beet, and wine cultures in the two first weeks of March [AGRESTE, Service Central d'Enquêtes et d'Études Statistiques, 2006]. Hamaoui-Laguel *et al.* [2014] indeed found an emission increase over the French region Champagne-Ardenne with respect to EMEP from February to April 2007. The  $\text{NH}_3$ -SAT emission pattern over Germany is consistent with the dynamic spring emissions of Danish Eulerian Hemispheric Model of Skjøth *et al.* [2011], the latter being driven by manure and fertilizer applications.

Finally, it should be noted that we also found that emissions decrease over some regions, as over the Po Valley (on 24 and 26–29 March 2012 and on 13 and 14 March 2014, see Figure S4), being consistent with Van Damme *et al.* [2014b] and their comparison between IASI and the LOTOS-EUROS model and over western France, being in agreement with Hamaoui-Laguel *et al.* [2014].

### 4.2. Improvement of Simulated $\text{NH}_3$ Surface Concentrations Using IASI-Derived Emissions

The evaluation of  $\text{NH}_3$ -SAT emissions is done for March 2014 with the available  $\text{NH}_3$  measurements listed in Table S4. To evaluate the  $\text{NH}_3$ -SAT emissions and their significant impact on  $\text{NH}_3$  concentrations (see Figure 2b), we compared model simulations with independent  $\text{NH}_3$  measurements. As strong changes were obtained over Germany, we made the evaluation against weekly  $\text{NH}_3$  Mini-Denuder measurements for six German EMEP sites (Table 1). Except for the mountainous Schauinsland station, weekly  $\text{NH}_3$  concentrations simulated with  $\text{NH}_3$ -SAT emissions are higher than the ones simulated with EMEP. The highest improvements are seen at stations Schmuecke and Waldhof (bias reduction of, respectively, 95% and 34%) located over agricultural regions. However, at mountainous station Schauinsland or at coastal stations Westerland or Zingst, the improvement is small (bias reduction of, respectively, 10, 5, and 4%) and  $\text{NH}_3$ -SAT emissions still lead to insufficient  $\text{NH}_3$  concentrations levels. The main reason could certainly be the sharp selection of IASI data



**Table 1.** Statistical Comparison of Observed and Modeled  $\text{NH}_3$  Concentrations Using Both EMEP and  $\text{NH}_3$ -SAT Emissions, in  $\mu\text{g m}^{-3}$ , at Six German Sites, Two Czech Stations, and One Dutch Station<sup>a</sup>

Network	Site	Period	Obs	With EMEP				With $\text{NH}_3$ -SAT			
				Modeled	Bias	RMSE	<i>R</i>	Modeled	Bias	RMSE	<i>R</i>
German EMEP	Westerland	Week	2.8	0.8	2.0	-	-	<b>0.9</b>	1.9	-	-
	Schauinsland	Week	3.4	5.3	1.9	-	-	<b>5.1</b>	1.7	-	-
	Neuglobsow	Week	2.6	1.5	1.1	-	-	<b>1.7</b>	0.9	-	-
	Zingst	Week	4.3	1.7	2.6	-	-	<b>1.8</b>	2.5	-	-
	Schmuecke	Week	3.6	1.8	1.8	-	-	<b>3.7</b>	0.1	-	-
	Waldhof	Week	5.4	1.9	3.5	-	-	<b>3.1</b>	2.3	-	-
Czech	Ustecky	week	5.3	0.9	4.7	5.5	0.0	<b>2.4</b>	3.8	4.8	0.3
		8th	5.3	0.3	5.0	5.3	0.7	<b>4.8</b>	0.5	2.5	0.8
		14th	7.6	1.6	6.5	7.4	0.0	<b>8.0</b>	0.4	4.7	0.5
	Pardubice	week	6.7	0.8	5.9	6.3	0.3	<b>2.0</b>	4.7	5.7	0.4
		8th	6.4	0.3	6.0	6.4	0.8	<b>4.4</b>	2.0	2.8	0.8
		14th	9.3	1.5	7.8	8.1	0.0	<b>7.8</b>	1.3	6.0	0.0
MLM	Vredepeel-	week	44.5	8.3	36.2	43.2	0.2	<b>9.4</b>	35.0	42.3	0.2
	Vredeweg(131)	14th	50.6	7.9	42.7	43.3	0.7	<b>18.9</b>	31.7	32.3	0.8

<sup>a</sup>As the selected IASI super-observations provide information to deduce  $\text{NH}_3$ -SAT emissions only on these particular days over Czech Republic (see Figure 2), the evaluation is performed on 8 and 14 March 2014. Similarly, the evaluation is done for 14 March 2014 at Vredepeel-Vredeweg. The use of  $\text{NH}_3$ -SAT emissions improves the comparison with surface measurements at all sites (results highlighted in bold).

with uncertainty lower than 50%, which particularly provide information over agricultural regions, of interest here, during this particular week (see Figure 2a). Then, this criterion of low error does not allow IASI to constrain the emissions over mountainous or coastal regions.

This could also be explained, to a lesser extent, by a misrepresentation of deposition. Indeed, the parameterization of  $\text{NH}_3$  dry deposition is unidirectional in our model, as most of the models in the world, whereas ideally it should be bidirectional [Sutton *et al.*, 2007]. Wichink Kruit *et al.* [2012] include a bidirectional air-surface atmosphere exchange, using a compensation point for vegetation and also for water, in their regional chemistry transport model LOTOS-EUROS. This new parameterization increases their modeled European ammonia concentrations almost everywhere, and particularly over agricultural source areas (increase of about 20–40%) and over coastal regions (increase of at least 80%). Nevertheless, their comparison with IASI still leads to similar results as those presented here (see section 4.1). Moreover, the impact of such air-surface exchange on  $\text{NH}_3$  concentrations could be contradictory (decrease of  $\text{NH}_3$  emissions in the Northern Hemisphere modeled by Zhu *et al.* [2015] when the inclusion of a compensation point for vegetation is included in the Goddard Earth Observing System-Chemistry (GEOS-Chem) global CTM). Thus, further work needs to be done to better investigate the sensitivity of  $\text{NH}_3$  concentrations to the deposition.

An evaluation is also performed with hourly  $\text{NH}_3$  measurements from Ustecky and Pardubice stations in Czech Republic for 8 and 14 March 2014 and from Vredepeel-Vredeweg in the Netherlands for 14 (Table 1), when  $\text{NH}_3$ -SAT emissions are changed compared to the EMEP ones (see Figures S4 and S5). All the statistic indicators are improved with  $\text{NH}_3$ -SAT emissions for both stations. At Ustecky, on 8 March, mean bias is reduced from 5.0 to  $0.5 \mu\text{g m}^{-3}$ . At Vredepeel-Vredeweg, on 14 March, mean bias is reduced from 42.7 to  $32.7 \mu\text{g m}^{-3}$ . Moreover, and even if the diurnal temporal profile of  $\text{NH}_3$  emissions is not changed (as seen in Figure S5a), the mean spatiotemporal correlation between simulated and measured  $\text{NH}_3$  concentrations is also improved with  $\text{NH}_3$ -SAT emissions ( $r = 0.5$  against  $r = 0.0$  with EMEP at Ustecky,  $r = 0.8$  against  $r = 0.7$  with EMEP at Vredepeel-Vredeweg on 14).

Increase of  $\text{NH}_3$ -SAT emissions, leading to an increase and to a diurnal redistribution of  $\text{NH}_3$  concentrations, conducts to significant improvements of the comparison with surface measurements over Germany, Czech Republic, and the Netherlands.

#### 4.3. Improvement of Simulated Ammonium, Nitrate, and $\text{PM}_{2.5}$ Concentrations Using IASI-Derived Emissions

As  $\text{NH}_3$  plays a decisive role in the chemical formation of particulate matter, we analyzed the impact of a redistribution of  $\text{NH}_3$  emissions on ammonium, nitrate, and  $\text{PM}_{2.5}$  surface concentrations. Figure 2d

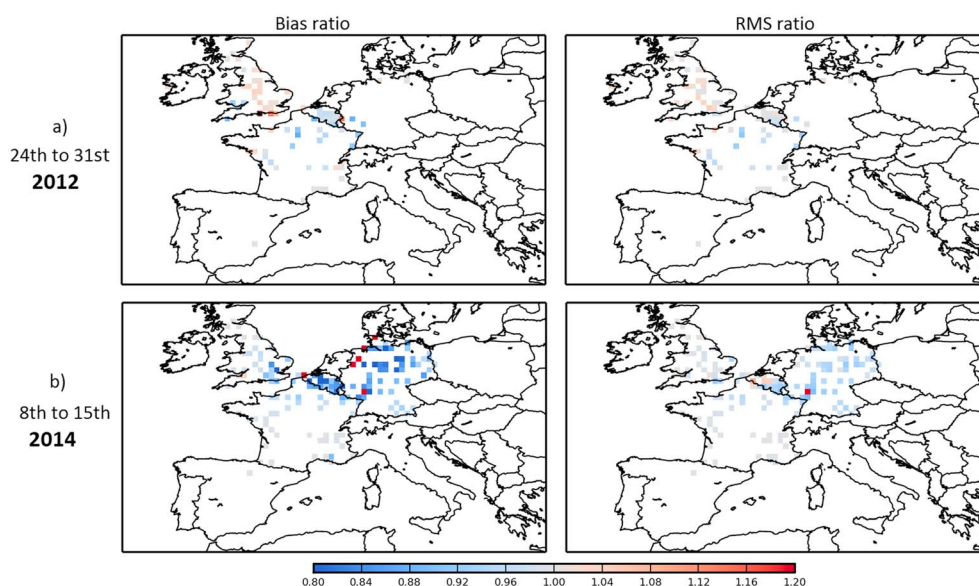


**Figure 3.** Ratios of mean bias and mean RMSE between  $\text{PM}_{2.5}$  concentrations simulated by CHIMERE using EMEP or  $\text{NH}_3$ -SAT emissions and  $\text{PM}_{2.5}$  AirBase measurements calculated as in equation (1) for (a) 24 to 31 March 2012 and (b) 8 to 15 March 2014. All ratios lower than 1, in blue, demonstrate that  $\text{NH}_3$ -SAT emissions improve the simulation compared to the EMEP simulation.

displays the relative differences between  $\text{PM}_{2.5}$  concentrations simulated by CHIMERE using EMEP and using  $\text{NH}_3$ -SAT emissions from 18 to 31 March 2012 and from 8 to 15 March 2014. Due to the increase of  $\text{NH}_3$ -SAT concentrations and consecutive, of ammonium nitrate concentrations (see Figures 2c and S6),  $\text{PM}_{2.5}$  concentrations can increase locally by about 30% over central Europe (see daily evolution in Figure S7).

First, we checked if the updated daily nitrate ( $\text{pNO}_3^-$ ) and ammonium ( $\text{pNH}_4^+$ ) surface levels better fit the observations from Revin station in eastern France from 8 to 15 March 2014 (Table S5), one of the only available station providing speciation measurements in our regions of interest (Germany and east of France). Consistently with the evaluation of  $\text{NH}_3$  concentrations (of section 4.2), nitrate and ammonium concentrations are underestimated in the both simulations (with EMEP and with  $\text{NH}_3$ -SAT). As  $\text{NH}_3$ -SAT emissions are only slightly modified in Revin, it has a low impact on nitrate and ammonium concentrations. Nevertheless, the daily biases are still reduced by around 10% with the use of  $\text{NH}_3$ -SAT emissions (excepted on 12 March 2014, with a bias reduction of 18%).

We then compared simulations using EMEP and  $\text{NH}_3$ -SAT emissions respectively with AirBase surface  $\text{PM}_{2.5}$  measurements with all types of stations (i.e., urban, rural, etc.). Mean weekly ratios from 24 to 31 March 2012 and from 8 to 15 March 2014 at the grid cell scale, displayed in Figure 3, are calculated as:

$$\text{Ratio} = \frac{\sum |\text{PM}_{2.5}\text{observations} - \text{model}(\text{withNH}_3 - \text{SATemissions})|}{\sum |\text{PM}_{2.5}\text{observations} - \text{model}(\text{withEMEPemissions})|} \quad (1)$$

It can be noticed that mean weekly bias and RMSE are significantly improved. All ratios being lower than 1 (in blue), it demonstrates that the use of  $\text{NH}_3$ -SAT emissions improves the simulation compared to the EMEP simulation. It can thus be concluded that mean weekly bias and RMSE are significantly improved, particularly over Germany, Belgium, and east of France. It is worth stressing that the modeled surface concentrations obtained with the updated emissions still present negative biases compared to the independent measurements. This underestimation of  $\text{PM}_{2.5}$ -simulated concentrations is a common feature of various models (CHIMERE, EMEP, and LOTOS-EUROS) [Hamaoui-Laguel et al., 2014; Bessagnet et al., 2014] and can be attributed to the underestimation of ammonium nitrate concentrations and also to factors other than ammonia emissions, such as underestimation of primary particulate matter emissions and possible misrepresentation in the modeling of aerosol formation.

Finally, the hourly correlation of  $\text{PM}_{2.5}$  surface concentrations is slightly improved with  $\text{NH}_3$ -SAT emissions for a large set of stations. As an example for the northeastern French stations where maximum  $\text{PM}_{2.5}$  concentrations were observed, the mean spatiotemporal correlation is increased by about 3% (respectively,  $r=0.8$  against  $r=0.7$  with EMEP). These results demonstrate the capability of IASI to provide useful information about  $\text{NH}_3$  emissions at a high spatiotemporal resolution and comfort preliminary observations of large spring  $\text{NH}_3$  emissions over central Europe.

## 5. Discussion and Conclusions

We report here on satellite derivation of daily ammonia emissions during the particulate matter pollution event of March 2012 and March 2014, using IASI total columns and the chemistry transport model CHIMERE. This emission inversion approach is based here on (i) relationships between  $\text{NH}_3$  surface emissions and total columns for low wind speed events and (ii) IASI  $\text{NH}_3$  super-observations and associated retrieval error lower than 50%. This current method has some limitations due to the assumption on weak transport from cell to cell. To extend it to a broader number of situations, accounting for transport out of grid cell is necessary for which variational inversion methods are well suited. These methods also allow the inclusion of a weighting procedure between a priori emissions and observations, by considering their respective errors (and therefore considering all IASI observations).

To our knowledge, this is the first time that satellite measurements of atmospheric ammonia are used to deduce daily  $\text{NH}_3$  emissions due to agricultural practices. IASI reveals highly variable  $\text{NH}_3$  emission distributions certainly due to fertilizer spreading occurring mainly over Germany and eastern France. These could differ with respect to the monthly mean a priori emissions by a factor up to 3, with most of the time increases diagnosed. Given the rather coarse model resolution (50 km in the horizontal, first model layer at about 40 m height), diagnosed emissions can be considered as net emissions, taking into account deposition very close to emissions sources. It is indeed net emissions, which need to be used as an input of continental scale air quality models. Use of satellite-derived  $\text{NH}_3$  emissions improved the comparison with independent  $\text{NH}_3$  surface measurements. Updating of  $\text{NH}_3$  emissions also significantly impacts and mostly increases  $\text{PM}_{2.5}$  concentrations, up to +30%. This shows (i) the need for accurate agricultural  $\text{NH}_3$  emissions, highly contributing to premature mortality in Europe and also in eastern USA, Russia, and East Asia [Lelieveld *et al.*, 2015] and (ii) the considerable potential of IASI space-based  $\text{NH}_3$  global distributions [Van Damme *et al.*, 2015b] to efficiently model and forecast particulate pollution episodes over these regions.

## References

- AGRESTE, Service Central d'Enquêtes et d'Études Statistiques (2006), Survey on agricultural practices for 2006.
- Bessagnet, B., et al. (2014), Can further mitigation of ammonia emissions reduce exceedances of particulate matter air quality standards?, *Environ. Sci. Policy*, 44, 149–163.
- Clarisse, L., C. Clerbaux, F. Dentener, D. Hurtmans, and P.-F. Coheur (2009), Global ammonia distribution derived from infrared satellite observations, *Nat. Geosci.*, 2, 479–483, doi:10.1038/ngeo551.
- Clerbaux, C., et al. (2009), Monitoring of atmospheric composition using the thermal infrared IASI/MetOp sounder, *Atmos. Chem. Phys.*, 9, 6041–6054, doi:10.5194/acp-9-6041-2009.
- European Monitoring and Evaluation Programme/European Environment Agency (2009), Emission inventory guidebook. [Available at <http://www.eea.europa.eu/publications/emep-eea-emission-inventory-guidebook-2009>, Uncertainties.pdf.]
- Erisman, J. W., A. Bleeker, A. Hensen, and A. Vermeulen (2008), Agricultural air quality in Europe and the future perspectives, *Atmos. Environ.*, 42, 3209–3217.
- Flechard, C. R., et al. (2011), Dry deposition of reactive nitrogen to European ecosystems: A comparison of inferential models across the NitroEurope network, *Atmos. Chem. Phys.*, 11, 2703–2728, doi:10.5194/acp-11-2703-2011.
- Hamaoui-Laguel, L., F. Meleux, M. Beekmann, B. Bessagnet, S. Genermont, P. Cellier, and L. Letinois (2014), Improving ammonia emissions in air quality modelling for France, *Atmos. Environ.*, 92, 584–595, doi:10.1016/j.atmosenv.2012.08.002.
- Hellsten, S., U. Dragosits, C. J. Place, M. Vieno, J. Dore, T. H. Misselbrook, Y. S. Tang, and M. A. Sutton (2008), Modelling the spatial distribution of ammonia emissions in the UK, *Environ. Pollut.*, 154(3), 370–379.
- Hertel, O., et al. (2012), Governing processes for reactive nitrogen compounds in the European atmosphere, *Biogeosciences*, 9, 4921–4954, doi:10.5194/bg-9-4921-2012.
- Hutchings, N., B. Amon, U. Dämmgen, and J. Webb (2009), EMEP/EEA emission inventory guidebook: Animal husbandry and manure management, *Tech. Rep.* 9/2009.
- Lelieveld, J., J. S. Evans, M. Fnais, D. Giannadaki, and A. Pozzer (2015), The contribution of outdoor air pollution sources to premature mortality on a global scale, *Nature*, 525, 367–371, doi:10.1038/nature15371.
- Menut, L., A. Goussebaile, B. Bessagnet, D. Kyvorostyanov, and A. Ung (2012), Impact of realistic hourly emissions profiles on air pollutants concentrations modelled with CHIMERE, *Atmos. Environ.*, 49, 233–244.
- Menut, L., et al. (2013), CHIMERE 2013: A model for regional atmospheric composition modelling, *Geosci. Model Dev.*, 6, 981–1028, doi:10.5194/gmd-6-981-2013.

### Acknowledgments

This study was funded by the French Space Agency-Centre National d'Études Spatiales CNES and by the European Commission under the EU Seventh Research Framework Programme (grant agreement 283576, MACC II). IASI has been developed and built under the responsibility of the "Centre National d'Études Spatiales" (CNES, France). It is flown on board the Metop satellites as part of the EUMETSAT Polar System. The IASI L1 data are received through the EUMETCast near real-time data distribution service. The research in Belgium was funded by the F.R.S.-FNRS, the Belgian State Federal Office for Scientific, Technical and Cultural Affairs (Prodex arrangement 4000111403 IASI.FLOW). M. Van Damme is grateful to the "Fonds pour la formation à la recherche dans l'industrie et dans l'agriculture" of Belgium for a PhD grant. L. Clarisse is research associate with F.R.S.-FNRS. C. Clerbaux is grateful to CNES for scientific collaboration and financial support. We gratefully acknowledge support from the project "Effects of Climate Change on Air Pollution Impacts and Response Strategies for European Ecosystems" (ÉCLAIRE), funded under the EC 7th Framework Programme (grant agreement 282910). The CHIMERE regional chemistry transport model and its technical documentation can be found here: [www.lmd.polytechnique.fr/chimere/](http://www.lmd.polytechnique.fr/chimere/). The European air quality database AIRBASE and its  $\text{PM}_{2.5}$  measurements can be found here: [www.eea.europa.eu](http://www.eea.europa.eu). Data for the Czech Republic were provided from the Czech Hydrometeorological Institute. We particularly thank Václav Novák for providing these  $\text{NH}_3$  surface measurements. We acknowledge the Dutch National Air Quality Monitoring Network for providing  $\text{NH}_3$  surface measurements and particularly thank Hans Berkhout from RIVM-Centre for Environmental Monitoring (MIL).



- Nenes, A., S. N. Pandis, and C. Pilinis (1999), Continued development and testing of a new thermodynamic aerosol module for urban and regional air quality models, *Atmos. Environ.*, **33**, 1553–1560.
- Petetin, H., J. Sciarre, M. Bressi, A. Rosso, O. Sanchez, R. Sarda-Estève, J.-E. Petit, and M. Beekmann (2015), Assessing the ammonium nitrate formation regime in the Paris megacity and its representation in the CHIMERE model, *Atmos. Chem. Phys. Discuss.*, **15**, 23,731–23,794.
- Skjøth, C. A., O. Hertel, S. Gyldenkaerne, and T. Ellerman (2004), Implementing a dynamical ammonia emission parameterization in the large-scale air pollution model ACDEP, *J. Geophys. Res.*, **109**, D06306, doi:10.1029/2003JD003895.
- Skjøth, C. A., T. Ellermann, O. Hertel, S. Gyldenkaerne, and M. H. Mikkelsen (2008), Footprints on ammonia concentrations from environmental regulations, *J. Air Waste Manage.*, **58**, 1158–1165.
- Skjøth, C. A., et al. (2011), Spatial and temporal variations in ammonia emissions—A freely accessible model code for Europe, *Atmos. Chem. Phys.*, **11**, 5221–5236, doi:10.5194/acp-11-5221-2011.
- Sutton, M. A., et al. (2007), Challenges in quantifying biosphere-atmosphere exchange of nitrogen species, *Environ. Pollut.*, **150**, 125–139, doi:10.1016/j.envpol.2007.04.014.
- Van Damme, M., L. Clarisse, C. L. Heald, D. Hurtmans, Y. Ngadi, C. Clerbaux, A. J. Dolman, J. W. Erisman, and P. F. Coheur (2014a), Global distributions, time series and error characterization of atmospheric ammonia ( $\text{NH}_3$ ) from IASI satellite observations, *Atmos. Chem. Phys.*, **14**, 2905–2922, doi:10.5194/acp-14-2905-2014.
- Van Damme, M., R. J. WichinkKruit, M. Schaap, L. Clarisse, C. Clerbaux, P.-F. Coheur, E. Dammers, A. J. Dolman, and J. W. Erisman (2014b), Evaluating four years of atmospheric ammonia ( $\text{NH}_3$ ) over Europe using IASI satellite observations and LOTOS-EUROS model results, *J. Geophys. Res. Atmos.*, **119**, 9549–9566, doi:10.1002/2014JD021911.
- Van Damme, M., et al. (2015a), Towards validation of ammonia ( $\text{NH}_3$ ) measurements from the IASI satellite, *Atmos. Meas. Tech.*, **8**, 1575–1591, doi:10.5194/amt-8-1575-2015.
- Van Damme, M., J. W. Erisman, L. Clarisse, E. Dammers, S. Whitburn, C. Clerbaux, A. J. Dolman, and P.-F. Coheur (2015b), Worldwide spatiotemporal atmospheric ammonia ( $\text{NH}_3$ ) columns variability revealed by satellite, *Geophys. Res. Lett.*, **42**, 8660–8668, doi:10.1002/2015GL065496.
- Vestreng, V. (2003), Review and Revision of Emission Data Reported to CLRTAP, EMEP Status Rep.
- von Bobatzki, K., et al. (2010), Field inter-comparison of eleven atmospheric ammonia measurement techniques, *Atmos. Meas. Tech.*, **3**, 91–112, doi:10.5194/amt-3-91-2010.
- Wichink Kruit, R. J., M. Schaap, F. J. Sauter, M. C. van Zanten, and W. A. J. van Pul (2012), Modeling the distribution of ammonia across Europe including bi-directional surface-atmosphere exchange, *Biogeosciences*, **9**, 5261–5277, doi:10.5194/bg-9-5261-2012.
- Xing, J., R. Mathur, J. Pleim, C. Hogrefe, C.-M. Gan, D. C. Wong, C. Wei, R. Gilliam, and G. Pouliot (2015), Observations and modeling of air quality trends over 1990–2010 across the Northern Hemisphere: China, the United States and Europe, *Atmos. Chem. Phys.*, **15**, 2723–2747, doi:10.5194/acp-15-2723-2015.
- Zhu, L., D. K. Henze, K. E. Cady-Pereira, M. W. Shepard, M. Luo, R. W. Pinder, J. O. Bash, and G.-R. Jeong (2013), Constraining U.S. ammonia emissions using TES remote sensing observations and the GEOS-Chem adjoint model, *J. Geophys. Res. Atmos.*, **118**, 3355–3368, doi:10.1002/jgrd.50166.
- Zhu, L., D. Henze, J. Bash, G.-R. Jeong, K. Cady-Pereira, M. Shephard, M. Luo, F. Paulot, and S. Capps (2015), Global evaluation of ammonia bidirectional exchange and livestock diurnal variation schemes, *Atmos. Chem. Phys.*, **15**, 12,823–12,843, doi:10.5194/acp-15-12823-2015.